Silicon Tubular Nanostructures

Synthesis of Crystalline Silicon Tubular Nanostructures with ZnS Nanowires as Removable Templates**

Junqing Hu, Yoshio Bando, Zongwen Liu, Jinhua Zhan, Dmitri Golberg, and Takashi Sekiguchi*

Since the discovery of carbon nanotubes in 1991,[1] a large number of inorganic solids with layered or nonlayered crystal lattices have been found to form stable and energetically viable nanotubes (composed of molecular layers) or tubular nanostructures.[2] Nowadays, inorganic nanotubes and tubular nanostructures with interesting properties and potential applications constitute an important domain of the nanostructural family. In particular, one-dimensional Si nanostructures are of special interest due to the key role of Si in the modern semiconductor industry. Different methods have been developed for the fabrication of Si nanowires, for example, the laser-ablation metal-catalytic method,[3] the oxide-assisted method,[4] and the solution technique.[5] There have also been reports on the synthesis of Si nanotubes, but these tubular forms of Si are either polycrystalline or amorphous.[6] Although the existence of stable monocrystalline Si nanotubes and tubular nanostructures has been predicted theoretically,[7] they have never been observed experimentally.

Among the many routes for synthesizing nanostructured materials, template-based methods offer various advantages.[8] Recently, monocrystalline GaN nanotubes were prepared by "epitaxial casting", in which hexagonal ZnO nanowires were used as templates for epitaxial overgrowth of thin GaN sheaths, and the ZnO nanowire templates were subsequently removed by thermal reduction and evaporation with formation of GaN tubular nanostructures.[9] We believed that this template process could be exploited to prepare monocrystalline Si tubular nanostructures. It is known that diamondlike cubic Si and zinc blende ZnS have similar crystal structures and very close lattice constants (ZnS: $a = 0.5431$ nm, Si: $a = 0.5420$ nm).[10] In accordance with lattice-matching theory, effective epitaxial growth of Si on ZnS substrates should be possible, since the growth of ZnS thin films on Si substrates has already been demonstrated.[11] Here we report on the growth of crystalline Si tubular nanostructures. A novel template process generates crystalline Si

[*] Dr. J. Hu, Dr. Y. Bando, Dr. Z. Liu, Dr. J. Zhan, Dr. D. Golberg, Dr. T. Sekiguchi
Advanced Materials Laboratory and Nanomaterials Laboratory
National Institute for Materials Science (NIMS)
Namiki 1-1, Tsukuba, Ibaraki 305-0044 (Japan)
Fax: (+81) 298-51-6280
E-mail: hu.junqing@nims.go.jp

[**] This work was supported by the Japan Society for the Promotion of Science (JSPS) Fellowship tenable at the National Institute for Materials Science, Tsukuba, Japan.

Supporting information for this article is available on the WWW under http://www.angewandte.org or from the author.

 DOI: 10.1002/ange.200352483

tubular nanostructures with outer diameters of about 60–180 nm, wall thicknesses of about 20–60 nm, and lengths of several micrometers. Zinc blende ZnS nanowires were used as one-dimensional templates for epitaxial growth of thin monocrystalline Si sheaths, which led to the formation of ZnS/Si core/shell nanowires. Crystalline Si tubular nanostructures were formed by chemical removal of the ZnS nanowire cores.

The X-ray diffraction pattern of a sample of Si tubular nanostructures is shown in Figure 1. The reflections can be indexed to diamondlike cubic Si with a lattice constant of $a = 5.428$ Å, consistent with the standard value (JCPDS file 27-1402: $a = 5.430$ Å) within experimental error.

The TEM images (Figure 2a–c) reveal that the product consists of relatively straight tubular structures. Typically, the lengths of the as-synthesized tubular structures can reach several micrometers. Most of them (Figure 2a) have outer

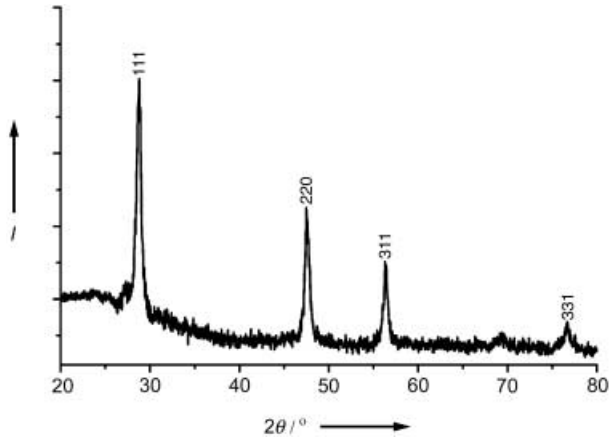

Figure 1. XRD pattern recorded from as-synthesized Si tubular nanostructures.

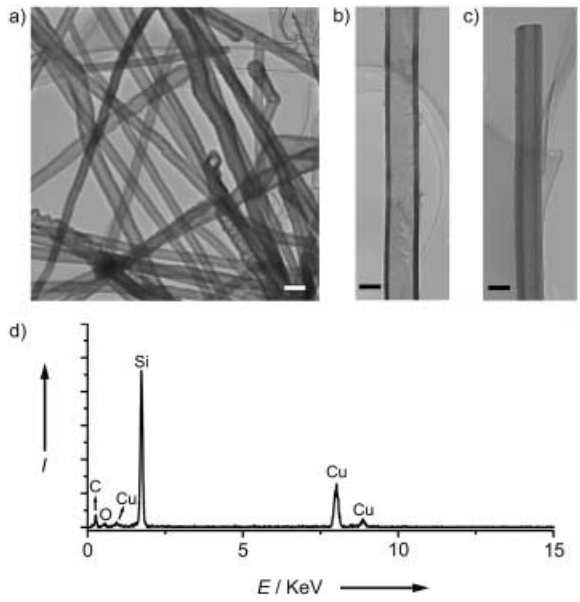

Figure 2. a) TEM image of Si tubular nanostructures. Scale bar: 200 nm. b) TEM image displaying an Si nanotube with a thin wall. c) TEM image displaying the open end of a Si nanotube. Scale bars in b) and c): 100 nm. d) EDS spectrum taken from an individual Si tubular nanostructure.

diameters of about 120–180 nm, and a small fraction of the tubes have smaller outer diameters of about 60–70 nm. The majority of tubes have wall thicknesses of about 40–60 nm, and a small number have thinner walls with thicknesses of about 20 nm (Figure 2b). Some tubes have one closed end (Figure 2a), while others are open-ended (Figure 2c). Analysis by energy-dispersive X-ray spectroscopy (EDS, Figure 2d) confirmed that the nanotubes are made of Si with a minimal content of O. Together with the XRD data, these results show that the obtained sample consists of crystalline Si tubular nanostructures.

Figure 3a shows a high-magnification TEM image of a segment of a straight Si tubular structure with an outer diameter and wall thickness of about 60 and 20 nm, respectively. The electron diffraction (ED) pattern (Figure 3a, inset) can be indexed to the [110] zone axis of crystalline Si, in which the streaking along the [111] direction originates from the stacking faults on the {111} planes, as suggested by the streaklike contrasts on the corresponding faces in TEM images. Figure 3b depicts the high-resolution TEM image of this crystalline tubular nanostructure, in which the (111) fringes with a d spacing of about 0.31 nm are aligned perpendicular to the longitudinal direction of the tube, suggesting a [111] growth orientation of the monocrystalline Si tubular domains. The thin sheath of amorphous SiO_2 that was noticed on the surface was attributed to unavoidable surface oxidation and/or surface adsorption of oxygen on the tubes during sample processing. Figure 3c and d respectively show a TEM image and its corresponding Si elemental map for a thin Si tubule. Line-scanning elemental profiles across the Si nanotube (white line in Figure 3c) representing the spatial distribution of the atomic species are shown in Figure 3e. The Si profile displays two peaks with a gap in the center. Both the elemental map and spatially resolved elemental profile show the tubular shape of the Si nanomaterial.

In the template-based growth of the crystalline Si tubular nanostructures, ZnS/Si core/shell nanowires were initially obtained, as shown in the TEM image in Figure 4a, in which the shell is a Si thin layer, and the core is a ZnS nanowire. As seen in Figure 4b, residual segments (nanorods) of the ZnS nanowire template remains in an open-ended Si tubular nanostructure after treatment of the ZnS/Si core/shell nanowires with HCl solution, owing to incomplete decomposition of the ZnS nanowire, which suggests that the Si tubular nanostructure is an extension of the thin Si sheath of the ZnS/Si core/shell nanowire. Figure 4c shows an HRTEM image of the interfacial domain between the Si shell and the ZnS core of a ZnS/Si core/shell nanowire. The well-defined epitaxial relationship ($(111)_{Si}//(111)_{ZnS}$; $[111]_{Si}//[111]_{ZnS}$) between the Si shell and ZnS core that is clearly observed is due to the similar crystal structure and the close lattice-matching of Si and ZnS. Line-scanning elemental profiles across a ZnS/Si core/shell nanowire (white line in Figure 4a) are shown in Figure 4d. The profile of Si shows two peaks, on the right- and left-hand sides, with lower intensity in the center, whereas the profiles of Zn and S both show a broad peak at the center; this verifies the core/shell nature of the ZnS/Si nanowires. It is noteworthy that polycrystalline Si nanotubes and microtubes were

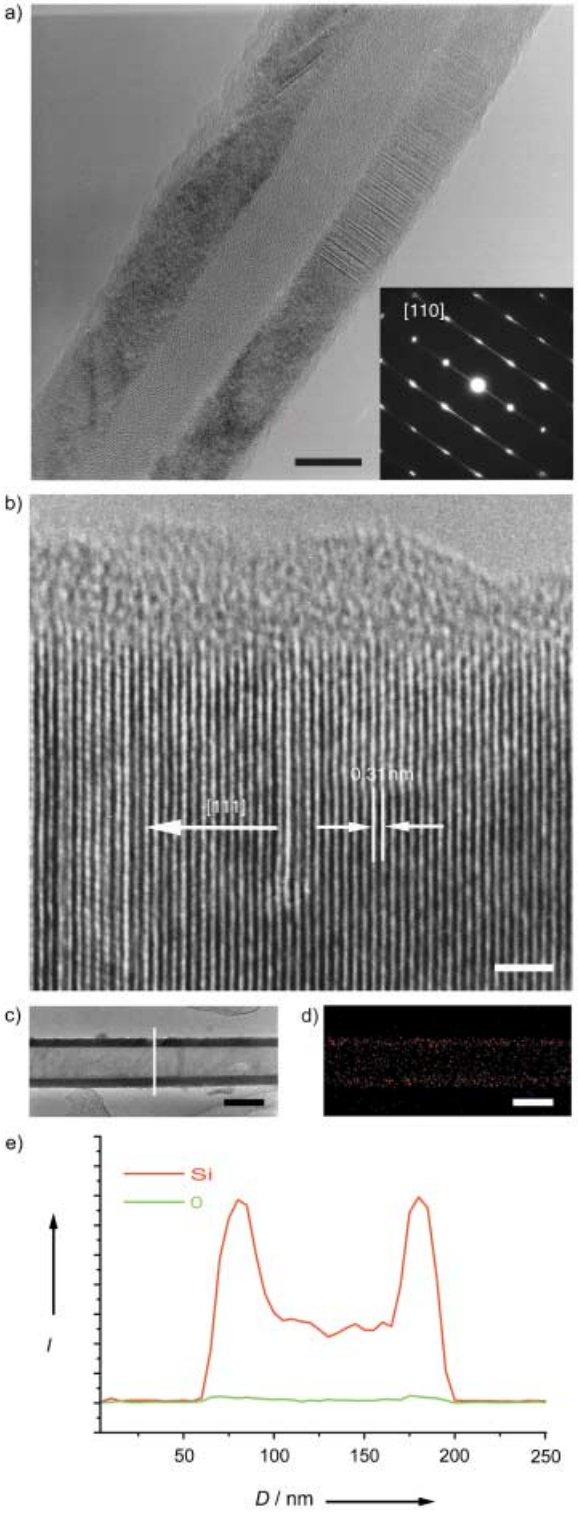

Figure 3. a) High-magnification TEM image depicting a segment of a Si nanotube, and an ED pattern (inset) corresponding to the [110] zone axis of a Si single crystal. Scale bar: 20 nm. b) HRTEM image of a Si nanotubular structure, in which the (111) (d_{111} = 0.31 nm) fringes are aligned perpendicular to the axis direction of the tube, which suggests a [111] growth direction of this tubular nanostructure. Scale bar: 2 nm. c) TEM image of a segment of a Si nanotube. d) Si elemental map as further evidence for a tubular structure. Scale bars in c) and d): 100 nm. e) Line-scanning (indicated by a line in c)) elemental mapping highlighting the spatial Si elemental profile across the tube.

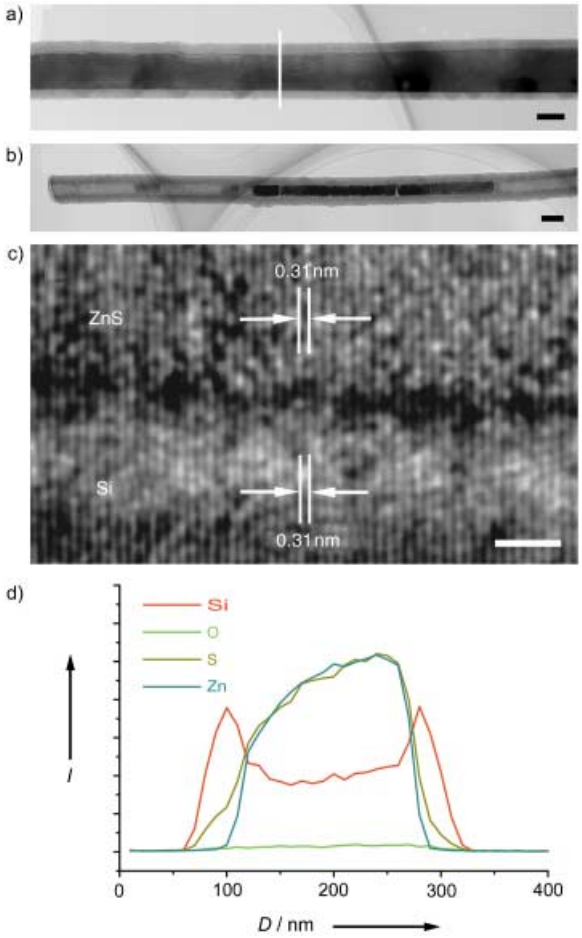

Figure 4. a) TEM image of a segment of a ZnS/Si core/shell nanowire. b) TEM image showing the residual segments of the ZnS nanowire template in the open-ended Si nanotube after treatment of the ZnS/Si core/shell nanowires with HCl solution. Scale bars in a) and b): 100 nm. c) HRTEM image taken from the interfacial domain between the Si shell and ZnS core of a ZnS/Si core/shell nanowire, revealing an epitaxial relationship ($(111)_{Si}//(111)_{ZnS}$; $[111]_{Si}//[111]_{ZnS}$) between the Si shell and the ZnS core. Scale bar: 2 nm. d) Line-scanning (indicated by a white line in a)) elemental mapping displaying Si, Zn, and S spatial elemental distribution profiles across the ZnS/Si core/shell nanowire.

obtained from similar synthetic processes in the absence of ZnS nanowire templates. This implies that the ZnS nanowires formed during the first stage of synthesis play the key role in producing monocrystalline Si tubular structures in the two-stage ZnS-nanowire-templated process.

Figure 5 shows a room-temperature cathodoluminescence (CL) spectrum of the Si tubular nanostructures. One broad and weak emission peak at about 450 nm was detected. Compared with the photoluminescence behavior of bulk Si nanowires (emission band centered at $\approx$624 nm (N_2 carrier gas) or $\approx$783 nm (Ar carrier gas)),[12] the peak position of the Si tubular nanostructures is shifted dramatically to lower wavelengths; this may be attributable to some intrinsic point defects and impurities in these Si nanostructures.

Monocrystalline Si tubular nanostructures are distinctly different from previously reported Si nanowires and other Si-based nanostructures,[13] due to the characteristic internal

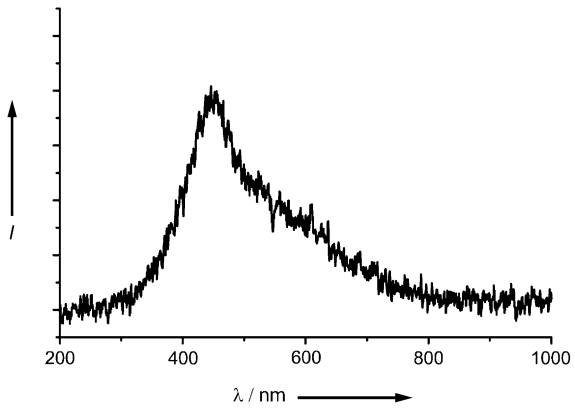

Figure 5. Room-temperature CL spectrum of the as-synthesized Si tubular nanostructures.

cavity peculiar to a tubular shape. This cavity could be filled with different semiconducting materials with various band gaps to give interesting electrical and optical nanodevices, for example, nanoscale lasers and/or light emitting devices with tunable wavelengths. In addition, theoretical predictions have indicated that Si nanotubes (or tubular nanostructures) have a semiconducting band gap, which in contrast to carbon nanotubes, is independent of the tube diameter or chirality.[7b] We believe that the present discovery of Si crystalline tubular nanostructures will promote further experimental studies on their physical properties and applications.

Experimental Section

ZnS/Si core/shell nanowires were grown by thermal evaporation of ZnS and SiO powders under controlled conditions in a vertical induction furnace, as described in detail elsewhere.[14] Briefly, the furnace consisted of a fused-quartz tube and an inductively heated cylinder made of high-purity graphite coated with a thermally insulating layer of carbon fiber. A graphite crucible containing ZnS powder was placed in the central cylindrical zone. After evacuation of the quartz tube to about 0.2 Torr, a stream of pure Ar was passsed through the tube at a flow rate of 120 $cm^3 s^{-1}$ and ambient pressure, and evaporation was conducted at 1200 °C (measured by an optical pyrometer with an estimated accuracy of ± 10 °C). Numerous ZnS nanowires with diameters of 20–60 nm had grown on the carbon-fiber layer after 1.5 h of evaporation. They were directly used as templates for the growth of ZnS/Si core/shell nanowires in the following stage of synthesis: The crucible containing SiO powder was rapidly heated to 1450 °C and maintained at this temperature for 1 h (the pressure in the tube and Ar flow rate in this stage were kept unchanged). The disproportionation of SiO led to the formation of Si vapor. A thin layer of Si grew by condensation of the Si vapor on the ZnS nanowire templates, and ZnS/Si core/shell nanowires formed. Finally, the ZnS nanowire templates were removed from the ZnS/Si core/shell nanowires with HCl solution. This final step resulted in the formation of crystalline Si tubular nanostructures. The collected products were characterized and analyzed by X-ray diffraction (XRD, RINT 2200), transmission electron microscopy (TEM, JEM-3000F and JEM-3100FFF), and energy-dispersive X-ray spectroscopy (EDS). Cathodoluminescence (CL) spectroscopy was carried out with a high-spatial-resolution, low-energy CL (HRLE-CL) system and a thermal field-emission scanning electron microscope (TFE-SEM, Hitachi S4200).

Received: July 28, 2003
Revised: September 12, 2003 [Z52483]

Keywords: crystal growth · epitaxy · nanostructures · nanotubes · silicon

[1] S. Iijima, *Nature* **1991**, *354*, 56.
[2] See, for example a) R. Tenne, L. Margulis, M. Genut, G. Hodes, *Nature* **1992**, *360*, 444; b) E. J. M. Hamilton, S. E. Dolan, C. M. Mann, H. O. Colijn, C. A. Mcdonald, S. G. Shore, *Science* **1993**, *260*, 659; c) Y. Feldman, E. Wasserman, D. J. Srolovitz, R. Tenne, *Science* **1995**, *267*, 222; d) N. G. Chopra, R. J. Luyken, K. Cherrey, V. H. Crespi, M. L. Cohen, S. G. Louie, A. Zettl, *Science* **1995**, *269*, 966; e) P. Hoyer, *Langmuir*, **1996**, *12*, 1411; f) R. Tenne, M. Homyonfer, Y. Feldman, *Chem. Mater.* **1998**, *10*, 3225; g) L. Pu, X. M. Bao, J. P. Zou, D. Feng, *Angew. Chem.* **2001**, *113*, 1538; *Angew. Chem. Int. Ed.* **2001**, *40*, 1490; h) E. J. Mele, P. Kral, *Phys. Rev. Lett.* **2002**, *88*, 056803-1; i) M. Nath, C. N. R. Rao, *Angew. Chem.* **2002**, *41*, 3601; *Angew. Chem. Int. Ed.* **2002**, *41*, 3451; j) J. H. Jung, H. Kobayashi, K. J. C. van-Bommel, S. Shinkai, T. Shimizu, *Chem. Mater.* **2002**, *14*, 1445.
[3] a) A. M. Morales, C. M. Lieber, *Science* **1998**, *279*, 208; b) Y. Cui, L. J. Lauhon, M. S. Gudiksen, J. F. Wang, C. M. Lieber, *Appl. Phys. Lett.* **2001**, *78*, 2214.
[4] a) N. Wang, Y. H. Tang, Y. F. Zhang, C. S. Lee, S. T. Lee, *Phys. Rev. B* **1998**, *58*, R16024; b) S. T. Lee, Y. F. Zhang, N. Wang, Y. H. Tang, I. Bello, C. S. Lee, Y. W. Chung, *J. Mater. Res.* **1999**, *14*, 4503; c) W. S. Shi, H. Y. Peng, L. Xu, N. Wang, Y. H. Tang, S. T. Lee, *Adv. Mater.* **2000**, *12*, 1927; d) J. L. Gole, J. D. Stout, W. L. Rauch, Z. L. Wang, *Appl. Phys. Lett.* **2000**, *76*, 2346.
[5] J. D. Holmes, K. P. Johnston, R. C. Doty, B. A. Korgel, *Science* **2000**, *287*, 1471.
[6] a) J. Sha, J. J. Niu, X. Y. Ma, J. Xu, X. B. Zhang, Q. Yang, D. R. Yang, *Adv. Mater.* **2002**, *14*, 1219; b) S. Y. Jeong, J. Y. Kim, H. D. Yang, B. N. Yoon, S.-H. Choi, H. K. Kang, C. W. Yang, Y. H. Lee, *Adv. Mater.* **2003**, *15*, 1172.
[7] a) S. B. Fagan, R. J. Baierle, R. Mota, A. J. R. da Silva, A. Fazzio, *Phys. Rev. B* **2000**, *61*, 9994; b) G. Seifert, T. Köhler, H. M. Urbassek, E. Hernández, T. Frauenheim, *Phys. Rev. B* **2001**, *63*, 193409; c) A. S. Barnard, S. P. Russo, *J. Phys. Chem. B* **2003**, *107*, 7577.
[8] See, for example a) W. Liang, C. R. Martin, *J. Am. Chem. Soc.* **1990**, *112*, 9666; b) C. J. Brumlik, C. R. Martin, *J. Am. Chem. Soc.* **1991**, *113*, 3174; c) R. Parthasarathy, C. R. Martin, *Nature* **1994**, *369*, 298; d) C. R. Martin, *Science* **1994**, *266*, 1961; e) M. Nishizawa, V. P. Menon, C. R. Martin, *Science* **1995**, *268*, 700; f) P. M. Ajayan, O. Stephan, P. Redlich, C. Colliex, *Nature* **1995**, *375*, 564; g) B. B. Lakshmi, P. K. Dorhout, C. R. Martin, *Chem. Mater.* **1997**, *9*, 857; h) J. C. Hulteen, C. R. Martin, *J. Mater. Chem.* **1997**, *7*, 1075.
[9] J. Goldberger, R. R. He, Y. F. Zhang, S. Lee, H. Q. Yan, H.-J. Choi, P. D. Yang, *Nature* **2003**, *422*, 599.
[10] S. M. Sze, *Physics of Semiconductor Devices*, Wiley-Interscience, New York, **1981**.
[11] a) L. T. Romano, R. D. Bringans, X. Zhou, W. P. Kirk, *Phys. B* **1995**, *52*, 11201; b) X. H. Zhou, S. Jiang, W. P. Kirk, *J. Appl. Phys.* **1997**, *82*, 2251; c) N. H. Tran, A. J. Hartmann, R. N. Lamb, *J. Phys. Chem. B* **2000**, *104*, 1150.
[12] Y. F. Zhang, Y. H. Tang, H. Y. Peng, N. Wang, C. S. Lee, I. Bello, S. T. Lee, *Appl. Phys. Lett.* **1999**, *75*, 1842.
[13] W. S. Shi, H. Y. Peng, N. Wang, C. P. Li, L. Xu, C. S. Lee, R. Kalish, S. T. Lee, *J. Am. Chem. Soc.* **2001**, *123*, 11095.
[14] a) D. Golberg, Y. Bando, L. Bourgeois, K. Kurashima, T. Sato, *Carbon* **2000**, *38*, 2017; b) D. Golberg, Y. Bando, W. Q. Han, K. Kurashima, T. Sato, *Chem. Phys. Lett.* **1999**, *308*, 337; c) W. Q. Han, Y. Bando, K. Kurashima, T. Sato, *Appl. Phys. Lett.* **1998**, *73*, 3085.

